Available online at www.sciencedirect.com

SciVerse ScienceDirect

Journal of the European Ceramic Society 32 (2012) 1283–1290

www.elsevier.com/locate/jeurceramsoc

Effects of the initial α-SiC content on the microstructure, mechanical properties, and permeability of macroporous silicon carbide ceramics

Jung-Hye Eom [a], Young-Wook Kim [a,*], In-Hyuck Song [b]

[a] *Functional Ceramics Laboratory, Department of Materials Science and Engineering, The University of Seoul, 90 Jeonnong-dong, Dongdaemun-ku, Seoul 130-743, Republic of Korea*

[b] *Engineering Ceramics Group, Korea Institute of Materials Science, 531 Changwondaero, Changwon, Gyeongnam 641-831, Republic of Korea*

Received 22 September 2011; accepted 26 November 2011
Available online 20 December 2011

Abstract

By using α- and/or β-SiC staring powders, the effects of the initial α-phase content on the microstructure, mechanical properties, and permeability of macroporous SiC ceramics were investigated. When β-SiC powder or a mixture of α/β powders containing a small amount (≤10%) of α-SiC powder was used, the microstructure consisted of large platelet grains. In contrast, when using α-SiC powder or α/β powders containing a large amount (>10%) of α powders, the microstructure consisted of small equiaxed grains. The development of large α-SiC platelet grains in the microstructure did not result in any improvement of the flexural strength of the macroporous SiC ceramics because of the accompanying pore growth and grain growth. The growth of the platelet-SiC grains was beneficial in increasing the gas permeability of the macroporous SiC ceramics from 4.12×10^{-13} m^2 for macroporous SiC with an equiaxed microstructure to 1.89×10^{-12} m^2 for macroporous SiC ceramics with large platelet grains.

Keywords: Sintering; Microstructure-final; Mechanical properties; SiC; Permeability

1. Introduction

Macroporous silicon carbide ceramics have many potential advantages including a low density, controlled permeability, high thermal shock resistance, high specific strength, excellent high temperature strength, and excellent corrosion resistance. These properties make the ceramics suitable for many applications such as molten metal filters, diesel particulate filters, gas burner media, gas sensors, vacuum chucks, preforms for metal–matrix composites, and lightweight structural materials.[1–21] The properties of macroporous SiC ceramics are strongly dependent on their porosity and microstructure. For example, an increase in porosity generally results in decreased mechanical strength[22–28] and increased permeability of macroporous SiC ceramics.[5,17,29,30] Moreover, macroporous SiC ceramics with smaller pores generally have a better flexural strength than ceramics with larger pores at an equivalent porosity.[31,32]

One way to control the microstructure of SiC ceramics is to adjust the initial α-SiC content in the starting composition. In dense liquid-phase sintered SiC ceramics, the use of β-SiC as a starting material results in a toughened microstructure consisting of platelet grains because of the β → α phase transformation and grain growth of SiC grains during sintering.[33] Meanwhile, the use of α-SiC as a starting material produces a microstructure consisting of equiaxed grains due to the stability of α-SiC at high temperatures.[34] SiC ceramics with a microstructure consisting of equiaxed grains are stronger than ceramics with a microstructure consisting of platelet grains. In contrast, SiC ceramics with platelet grains have a higher toughness than ceramics with a microstructure consisting of equiaxed grains.[33,35] However, the effect of the microstructure on the mechanical properties and permeability in macroporous SiC ceramics has not been systematically investigated.

Reports analyzing the permeability of macroporous SiC ceramics are quite limited.[9,17,30] Previous studies of the permeability of porous SiC ceramics suggest that permeability generally increases with increasing porosity. However, the effect of the microstructure on the permeability at an equivalent porosity has not been investigated in macroporous SiC ceramics.

* Corresponding author. Tel.: +82 2 2210 2760, fax: +82 2 2215 5863.
E-mail address: ywkim@uos.ac.kr (Y.-W. Kim).

0955-2219/$ – see front matter © 2011 Elsevier Ltd. All rights reserved.
doi:10.1016/j.jeurceramsoc.2011.11.040

In the present study, macroporous SiC ceramics with various microstructures ranging from a microstructure consisting of equiaxed grains to a microstructure consisting of platelet grains were produced by sintering using α-and/or β-SiC powders. The effects of the microstructure on the mechanical properties and permeability of macroporous SiC ceramics were investigated. A sintering additive with a composition in the Al_2O_3–Y_2O_3 (AY) system was selected because of its effectiveness in the development of an in situ-toughened microstructure[33] as well as its potential for improved strength.[18]

2. Experimental procedure

The following raw materials were used in this study: β-SiC (∼1.7 μm, B-hp, H.C.Starck, Berlin, Germany), α-SiC (∼0.45 μm, A-1, Showa Denko, Tokyo, Japan), Al_2O_3 (99.9% pure, Sumitomo Chemical Co., Tokyo, Japan), Y_2O_3 (99.9% pure, H.C. Starck GmbH & KG, Goslar, Germany) powders, and poly(methyl methacrylate-co-ethylene glycol dimethacrylate) microbeads (hereafter, microbeads, ∼8 μm, Sigma–Aldrich Inc, St. Louis, MO, USA) as a template. Six batches of powder were mixed (Table 1), each containing 60 wt% SiC (α and/or β), 5 wt% Al_2O_3–Y_2O_3 (AY) additives at a weight ratio of 3:2, and 35 wt% microbeads. In addition, two batches of powder containing 7 wt% additives with the same composition were prepared (Table 1) to investigate the effect of the sintering additive content. All individual batches were milled in ethanol for 24 h using SiC grinding balls after the addition of 4 wt% poly(ethylene glycol) as an organic binder. The milled slurry was dried, sieved, and pressed uniaxially under 50 MPa to produce rectangular bars. The compacts formed were heat-treated at 1000 °C for 1 h under argon at a heating rate of 1 °C/min to decompose the microbeads. The heat-treated samples were sintered at 1950 °C for 4 h in argon.

The bulk density of each macroporous ceramic was calculated from its weight-to-volume ratio. The porosity was then calculated as the ratio of the bulk density to the true density. The microstructures of the samples were observed by scanning electron microscopy (SEM). The grain size and pore size were measured from the SEM micrographs. X-ray diffraction (XRD) was performed on the ground powders using CuKα radiation.

Table 1
Batch composition of macroporous SiC ceramics.

Sample designation	Composition (wt%)				
	β-SiC[a]	α-SiC[b]	Al_2O_3	Y_2O_3	Microsphere[c]
0A5AY	60	0	3	2	35
1A5AY	59.4	0.6	3	2	35
3A5AY	58.2	1.8	3	2	35
10A5AY	54	6	3	2	35
50A5AY	30	30	3	2	35
100A5AY	0	60	3	2	35
0A7AY	58	0	4.2	2.8	35
1A7AY	57.4	0.6	4.2	2.8	35

[a] ∼1.7 μm, B-hp, H. C. Starck, Berlin, Germany.
[b] ∼0.45 μm, A-1, Showa Denko, Tokyo, Japan.
[c] ∼8 μm, poly(methyl methacrylate-co-ethylene glycol dimethacrylate) microbeads, Sigma–Aldrich Inc, St. Louis, MO, USA.

For the flexural strength measurements, bar-shaped samples were cut and polished to a size of 4 mm × 5 mm × 30 mm. Bend tests were performed at a crosshead speed of 0.5 mm/min using a three-point bending fixture with a span of 20 mm. The fracture toughness was measured by a single-edge notched beam (SENB) method.[36] The permeability was measured by a capillary flow porometer (CFP-1100-AEX, PMI), and the gas permeability (α) was computed from the measured flow rate and pressure difference using Darcy's law,

$$\frac{\Delta p}{L} = \frac{\eta \cdot Q}{A \cdot \alpha} \quad (1)$$

where Δp is the pressure drop from the entrance to the exit of the sample, L is the thickness of the sample, Q is the flow rate of air through the sample, η is the viscosity of air, A is the cross-sectional area of the sample, and α is the permeability. Samples with dimensions of 3 mm × 30 mm × 25 mm were fixed in a filter sample holder with an O-ring and adhesive. Based on Eq. (1), the permeability was calculated from the slope of the line of the plot of Δp vs. Q.

3. Results and discussion

3.1. Microstructure

The XRD analysis of the samples showed that the 0A5AY, 1A5AY, and 3A5AY samples consisted of 4H (α-SiC) as a major phase and 6H (α-SiC) as a minor phase. In contrast, the 50A5AY and 100A5AY samples were composed of 6H as a major phase and 4H as a minor phase, indicating the occurrence of the 3 C (β-SiC) → 4H phase transformation of SiC during sintering in the presence of the Al_2O_3–Y_2O_3 additive. In the case of 50A5AY and 100A5AY, the polytype of the starting α-SiC powder was 6H, resulting in 6H as a major phase.

Fig. 1 shows typical fracture surfaces of the macroporous SiC ceramics sintered at 1950 °C. The microstructure of the macroporous SiC ceramics fabricated from β-SiC (0A5AY) or β-SiC containing a small amount (≤10%) of α-SiC (1A5AY, 3A5AY, and 10A5AY) consisted of platelet grains. When the α content was increased from 0 to 10%, the size of the platelet grains decreased from 20–30 μm to 5–8 μm. In contrast, the microstructure of the ceramics fabricated from α-SiC (100A5AY) or β-SiC containing a large amount (50%) of α-SiC (50A5AY) consisted mostly of fine, equiaxed grains with a grain size of 2–5 μm. In general, the grain size decreased as the α-SiC content increased and the shape of the grains changed from platelet to equiaxed grains. These results suggest that the α-SiC particles acted as seeds for the grain growth of platelet SiC grains, which was accelerated by the β → α phase transformation of SiC, even though the particle size (∼0.45 μm) of α-SiC was smaller than that of the β-SiC particles (∼1.7 μm). When the amount of α-SiC particles added to β-SiC was increased from 1 to 10 wt%, the number of growing grains increased as a result of α-SiC seeding during sintering at a temperature as high as 1950 °C, at which α-SiC is considered a more stable phase than β-SiC. The increased number of growing grains led to smaller grains in the final microstructure because of impingement of

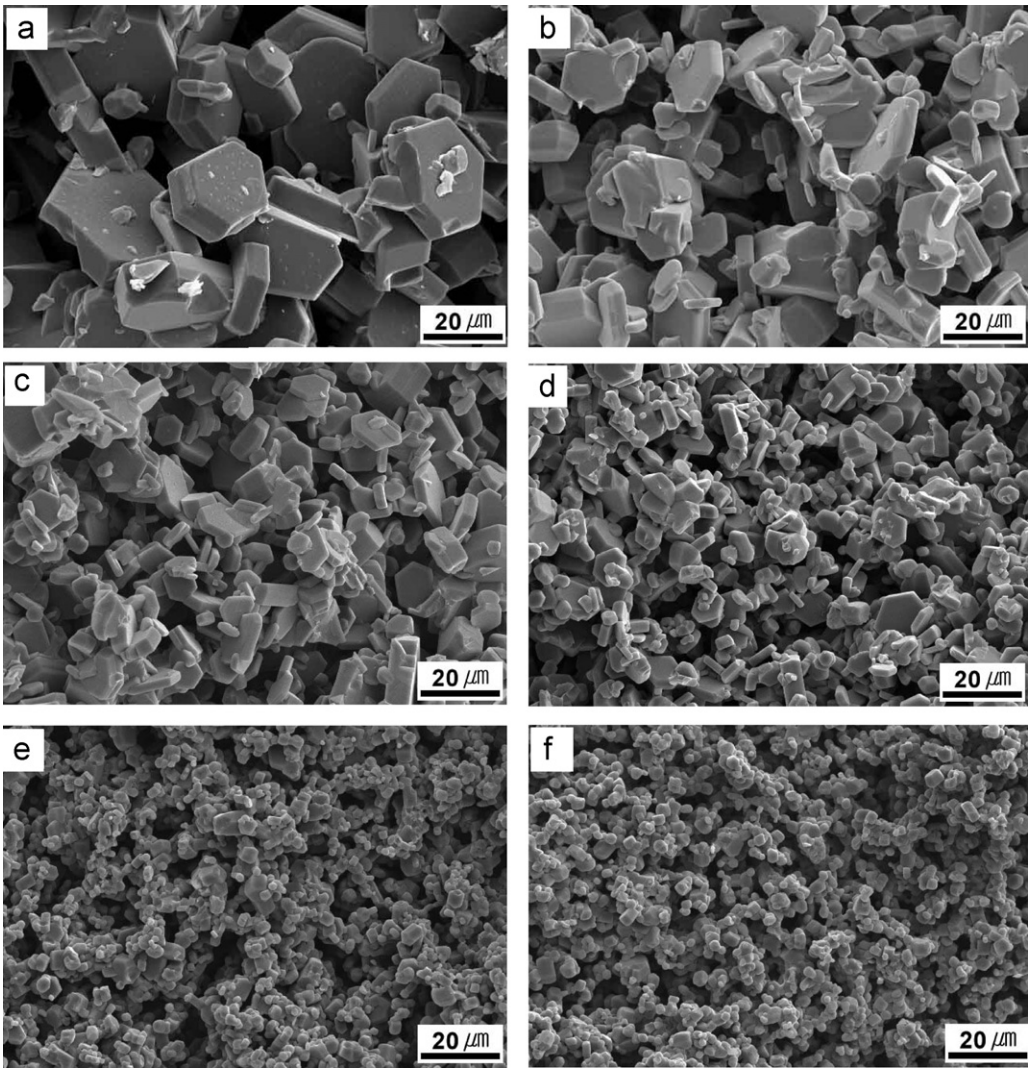

Fig. 1. Typical fracture surfaces of the macroporous SiC ceramics sintered at 1950 °C for 4 h in argon: (a) 0A5AY, (b) 1A5AY, (c) 3A5AY, (d) 10A5AY, (e) 50A5AY, and (f) 100A5AY (refer to Table 1).

the growing grains.[37] Therefore, 50% α-SiC addition resulted in considerably smaller grains, as shown in Fig. 1(e). The fine, equiaxed microstructure of the macroporous SiC ceramics fabricated from 100% α-SiC confirmed that the absence of the β → α phase transformation of SiC resulted in equiaxed grains.[38] This suggests that the microstructure of macroporous SiC ceramics can be adjusted by changing the α-phase content in the starting powder, as in the case of dense SiC ceramics.[33]

In previous work,[30,32,39] cells replicated from microbeads were almost spherical when polymer microbeads were added as a template into the SiC powders and polysiloxane-derived SiC ceramics. On the other hand, the cell morphologies of macroporous SiC ceramics fabricated from β-SiC (0A5AY) or β-SiC containing small amounts (≤10%) of α-SiC (1A5AY, 3A5AY, and 10A5AY) were mostly irregular. This was caused by the accelerated grain growth of platelet α-SiC grains during sintering. In turn, the accelerated grain growth of platelet α-SiC grains was caused by both the β → α phase transformation of SiC and the higher sintering temperature (1950 °C) used compared to previous studies (1700–1900 °C).[30,32,39] In contrast, the 50A5AY and 100A5AY samples maintained the spherical morphology of the cells replicated from the microbeads because less grain growth occurred compared to the other samples. Although the cell morphology and cell size were different, all samples had an interconnected open-cell structure.

The porosities of the 0A5AY, 1A5AY, 3A5AY, 10A5AY, 50A5AY, and 100A5AY samples were 58.4%, 57.3%, 56.5%, 56.4%, 56.0%, and 55.7%, respectively. The porosity of the macroporous SiC ceramics decreased with increasing α-phase content in the starting composition. The marked growth of large, platelet grains increased the porosity slightly because of the structural impingement of the growing grains in the microstructure.

Fig. 2 shows the change of the grain size and pore size as a function of the α-SiC content in the starting composition. The grain size decreased with increasing α content in the starting powder, indicating the growth of the added α-SiC particles. The samples prepared from β-SiC powders had the largest grain size among the samples investigated, and the addition of a small amount of α-SiC dramatically decreased the grain size because

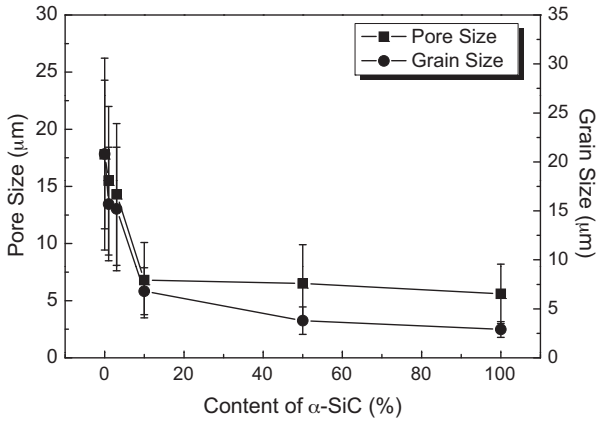

Fig. 2. Change in the grain size and pore size of macroporous SiC ceramics as a function of the α-SiC content in the starting powder.

of steric hindrance of the growing grains. The average grain size of the sample prepared from β powders (0A5AY) was ~21 μm, whereas that of the sample prepared from α powders (100A5AY) was ~3 μm. This same tendency has also been observed in dense SiC ceramics[33] and porous SiC ceramics sintered with Al_2O_3–Y_2O_3–CaO additives.[18] The pore size also decreased with increasing α content in the starting powder. It is well documented that grain growth generally accompanies the growth of pores in macroporous SiC ceramics.[40,41] Thus, with increasing α particle content, the grain growth of SiC grains is hindered by increasing impingement, resulting in a decreased pore size (Fig. 2) and more equiaxed grains (Fig. 1).

To understand the effect of the additive content, two samples (0A7AY and 1A7AY) sintered with 7 wt% Al_2O_3–Y_2O_3 additives were prepared and their microstructures are shown in Fig. 3. Like the samples containing 5 wt% Al_2O_3–Y_2O_3 sintering additive, the sample prepared from β powders (0A7AY) had a larger grain size than the sample prepared from β-SiC containing 1% α-SiC (1A7AY). The average grain size of the sample sintered with 7 wt% additives (0A7AY) was ~24 μm, whereas that of the sample sintered with 5 wt% additives (0A5AY) was ~21 μm. In contrast, the pore size decreased from 17.8 μm for the 0A5AY sample to 15.2 μm for the 0A7AY sample with increased additive content. A higher amount of sintering additives with the same composition led to the growth of larger platelet grains and decreased pore size, as is evident when comparing Fig. 1(a) and (b) and Fig. 3(a) and (b). Thus, a higher additive content led to a coarser microstructure with larger SiC grains. This result is explained by the reduced impingement of the growing SiC grains when more additives, i.e., more liquid were added. The same tendency has also been observed in dense SiC ceramics.[42] The porosities of the samples sintered with 7 wt% additives were 55.4% for 0A7AY and 54.7% for 1A7AY, which are slightly lower than those of the samples sintered with 5 wt% additives (58.4% for 0A5AY and 57.3% for 1A5AY). This was due to the enhanced densification of the samples containing a larger amount of additives.

3.2. Mechanical properties

Fig. 4 depicts the variation in flexural strength and fracture toughness as a function of the α-SiC content in the starting composition where each sample had a different microstructure. The flexural strength increased rapidly from 15 MPa to 21 MPa as the α-SiC content was increased from 0% to 10%. Then, the flexural strength increased gradually from 21 MPa to 26 MPa as the α-SiC content was increased from 10% to 100%. The pore size decreased rapidly from 18 μm to 7 μm as the α-SiC content was increased from 0% to 10% and then, the pore size was almost constant (6–7 μm) as the α-SiC content was increased from 10% to 100% (Fig. 2). The grain size decreased rapidly from 21 μm to 7 μm as the α-SiC content increased from 0% to 10%, and then the grain size decreased slowly from 7 μm to 3 μm as the α-SiC content was increased from 10% to 100% (Fig. 2). Increasing the α-SiC content in the starting composition from 0% to 10% was accompanied by a slight decrease in porosity from 58.4% to 56.4%, a decrease in grain size from ~21 μm to ~7 μm, and a decrease in pore size from ~18 μm to ~7 μm. Previous results showed that the strength of macroporous ceramics increases with decreasing porosity[19] and decreasing pore size.[32] Since the porosity decrease was small (~2%), the rapid increase in flexural strength with increasing α-SiC content from 0 to 10 wt% is likely to have been caused mainly by the decreased grain size and decreased pore size. The gradual increase in flexural strength with increasing α-SiC content from 10 to 100 wt% may be caused by a combination of the decrease in grain size from 7 μm to 3 μm, the decrease in porosity from 56.4% to 55.7%, and the decrease in pore size from 7 μm to 6 μm.The typical flexural strength of macroporous, polysiloxane-derived

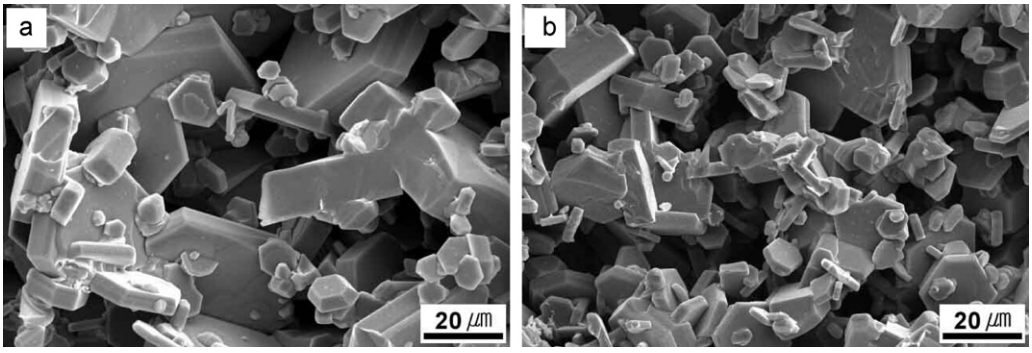

Fig. 3. Typical fracture surfaces of the macroporous SiC ceramics sintered with 7 wt% Al_2O_3–Y_2O_3 additives: (a) 0A7AY and (b) 1A7AY (refer to Table 1).

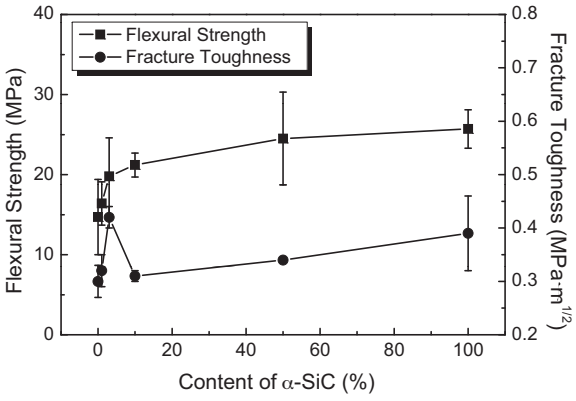

Fig. 4. Flexural strength and fracture toughness of macroporous SiC ceramics as a function of the α-SiC content in the starting powder.

SiC ceramics with an equiaxed microstructure was reported to be 22 MPa at a porosity of 52%.[43] Flexural strengths of 10 MPa and 14 MPa at porosities of 47% and 50%, respectively, were also reported in porous reaction-bonded SiC ceramics[44] and porous mullite-bonded SiC ceramics,[45] respectively. The flexural strength of the 100A5AY sample in the present study was 26 MPa at a porosity of 56%. In contrast, the flexural strength of the 0A5AY sample was 15 MPa at a porosity of 58%. Thus, comparison of the flexural strength of the two samples suggests that the development of large α-SiC platelet grains in the microstructure offers no improvement in flexural strength of the macroporous SiC ceramics because of the accompanying pore growth and grain growth. The present results also suggest that an equiaxed microstructure is beneficial in improving the strength of macroporous SiC ceramics fabricated from SiC powders. The strength of the 100A5AY sample (26 MPa at a porosity of 56%) is superior to or comparable to previously reported values.[43–45]

As shown in Fig. 4, the fracture toughness showed different behavior than that of the flexural strength as the α-SiC content in the starting composition was increased. The maximum toughness (0.42 MPa $m^{1/2}$) was obtained for the sample containing 3 wt% α-SiC. Initially, the toughness increased from 0.30 MPa $m^{1/2}$ to 0.42 MPa $m^{1/2}$ as the α-SiC content in the starting composition was increased to 3 wt%. But, at a 3 wt% α-SiC content, the toughness reached its maximum and decreased to 0.31–0.39 MPa $m^{1/2}$ at 10–100 wt% α-SiC content.Generally, the fracture toughness of liquid-phase sintered SiC ceramics increases with the development of platelet α-SiC grains but when the size of the platelet α-SiC grains becomes too large (>20 μm), the fracture toughness decreases with increasing grain size because of the increased likelihood of the transgranular fracture.[46] The maximum toughness obtained at 3 wt% α-SiC may be related to the optimal grain size (average grain size = 15.2 μm) of the sample. When the α-SiC content was higher than 3 wt%, the average grain size was in the range of 3–7 μm. In contrast, when no α-SiC was added, the average grain size was ~21 μm. Thus, it seems there is an optimum grain size for maximizing the toughness of the macroporous SiC ceramics, which may be dependent on the chemistry of the sintering additives, as in the case of dense SiC ceramics.[47–49]

The fracture toughness of porous SiC ceramics with a grain size of 2.5 μm and a porosity of 36.4% was reported to be 0.90 MPa $m^{1/2}$ and that of porous SiC ceramics with a grain size of ~0.5 μm and a porosity of 35.5% was 1.42 MPa $m^{1/2}$.[50] The fracture toughness of porous SiC ceramics derived from wood was previously reported to be 0.90–1.35 MPa $m^{1/2}$ in the axial direction and 0.23–0.60 MPa $m^{1/2}$ in the non-axial direction, depending on the porosity.[51] The fracture toughness generally decreases with increasing porosity.[51] A comparison of the fracture toughness values obtained in this study with values in the literature indicates that the toughness values we obtained are lower than the previously reported values. A crack-tip blunting mechanism contributes to the toughening of porous ceramics,[50] and the growth of platelet SiC grains in the porous SiC ceramics formed sharp edges and V-shaped notches (at the contacting region of two platelet grains) in the pores (see Fig. 1). The formation of sharp edges and V-shaped notches in the pore surfaces hindered the contribution of the crack bunting mechanism in the porous ceramics, resulting in lower fracture toughness. The present results suggest that the development of large α-SiC platelet grains in the macroporous SiC ceramics offers no improvement in fracture toughness, unlike dense SiC ceramics with a toughened microstructure.

3.3. Permeability

Fig. 5 shows the specific flow rate of macroporous SiC ceramics sintered at 1950 °C for 4 h. The specific flow rates of the 0A5AY, 1A5AY, and 100A5AY samples at a Δp of 15 psi were 23.3 L/min/cm^2, 12.7 L/min/cm^2, and 3.3 L/min/cm^2, respectively. The flow rate of the macroporous SiC ceramics increased with decreasing α-SiC content in the starting composition. The 0A5AY sample, which had a porosity of 58.4%, consisted of large platelet α-SiC grains (Fig. 1(a)), whereas the 100A5AY sample, which had a porosity of 55.7%, consisted of relatively small equiaxed α-SiC grains (Fig. 1(f)). The specific flow rate of the 0A5AY sample (23.3 L/min/cm^2) was seven times higher than that of the 100A5AY sample (3.3 L/min/cm^2), although the difference in their porosities was small (2.7%). In

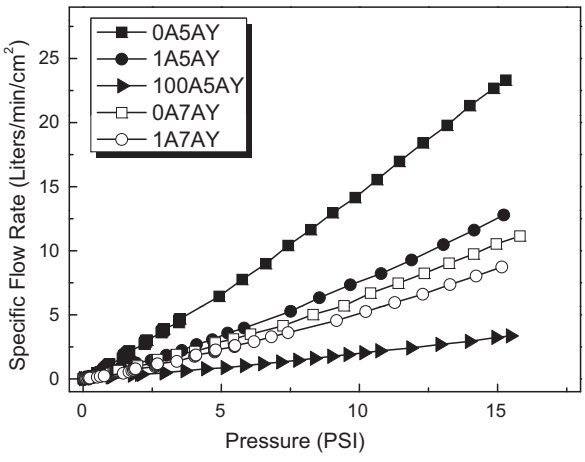

Fig. 5. Specific flow rate of macroporous SiC ceramic as a function of the pressure drop.

addition, the 1A7AY sample had a slightly lower porosity (54.7%) than the 100A5AY sample (55.7%), but the 1A7AY sample had a higher flow rate (8.7 L/min/cm^2) than the 100A5AY sample (3.3 L/min/cm^2) because of the development of large platelet α-SiC grains (see Fig. 3(b) and Fig. 1(f)). These results suggest that the development of large platelet α-SiC grains played an important role in improving the specific flow rate of macroporous SiC ceramics. This is also supported by a previous study of microcellular SiC ceramics with a duplex microstructure.[30] A specific flow rate of 6 L/min/cm^2 was reported for the ceramics in which the porosity was as high as 75% and the strut consisted of equiaxed grains.[30] Although the microcellular SiC ceramics had a higher porosity (75%) than the 0A5AY sample (~58%), the flow rate of the sample was 1/4 that of the 0A5AY sample.

To understand the effect of porosity and pore size on permeability, both the specific flow rate and pore size were plotted as a function of porosity (Fig. 6(a)). In addition, both the specific flow rate and porosity were plotted as a function of pore size (Fig. 6(b)). As shown in Fig. 6(a), both the specific flow rate and pore size increased with increasing porosity from 55.7% to 57.3%, and the porosity dependency of both properties was the same (both lines are parallel in Fig. 6(a)) within the above porosity range. However, a deviation from the parallelism was observed when the porosity was further increased

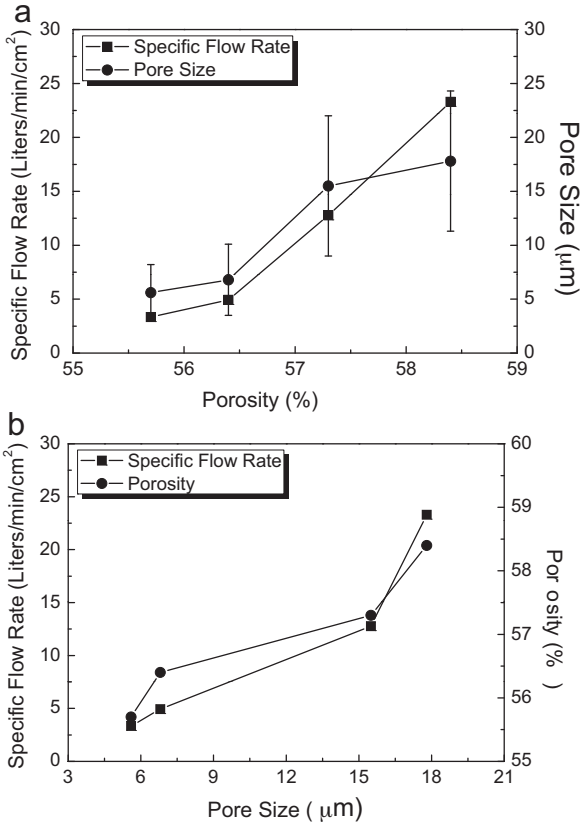

Fig. 6. (a) The permeability and pore size of macroporous SiC ceramics as a function of the porosity. (b) The permeability and porosity of macroporous SiC ceramics as a function of pore size.

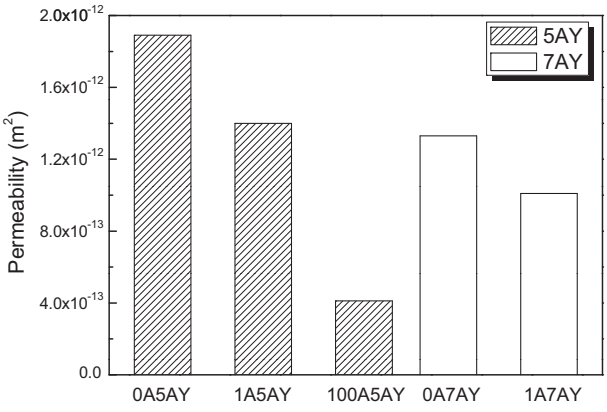

Fig. 7. Air permeability of macroporous SiC ceramics sintered at 1950 °C for 4 h.

from 57.3% to 58.4%. The specific flow rate increased continuously with increasing porosity up to 58.4%, whereas the pore size remained almost constant with increasing porosity from 57.3% to 58.4%. In Fig. 6(b), both the specific flow rate and porosity increased similarly with increasing pore size. These findings indicate that, in the porosity range of 55–60%, the specific flow rate is primarily dependent on the porosity rather than the pore size.

As shown in Fig. 5, the specific flow rates of the 0A7AY and 1A7AY samples were 11.1 L/min/cm^2 and 8.7 L/min/cm^2, respectively, at a Δp of 15 psi. The porosities of the 0A7AY and 1A7AY samples were 55.4% and 54.7%, respectively, and their pore sizes were 15.2 and 11.0 μm, respectively. The addition of more Al_2O_3–Y_2O_3 additive resulted in a decreased flow rate because of the decreased porosity and decreased pore size.

The permeabilities of the macroporous SiC ceramics are shown in Fig. 7. The permeabilities of the 0A5AY, 1A5AY, and 100A5AY samples were 1.9×10^{-12} m^2, 1.4×10^{-12} m^2, and 4.1×10^{-13} m^2, respectively. From Eq. (1), it is clear that the permeability is proportional to the flow rate. Permeability data for macroporous SiC ceramics is quite limited. Ding et al.[9] reported permeability values in the range of 10^{-13} m^2 for macroporous mullite-bonded SiC ceramics with a porosity ranging from 45% to 57%. Song et al.[30] reported permeability values in the range of 10^{-13} m^2 for macroporous SiC ceramics with a porosity of 75%. Although the porosities of the 0A5AY and 1A5AY samples were 58.4% and 57.3%, respectively, the permeability values (1.9×10^{-12} m^2 and 1.4×10^{-12} m^2) of the 0A5AY and 1A5AY samples were higher than the values reported in the literature at both a similar porosity as well as a higher porosity of up to 75% because of the beneficial effect of the large platelet SiC grains. However, Fukushima et al.[17] reported the highest permeability in the range of 10^{-11}–10^{-10} m^2 for highly porous SiC ceramics with a total porosity of 86%. This suggests that porosity is an important parameter for improving the permeability of macroporous SiC ceramics. However, at the same porosity, the development of large platelet SiC grains is beneficial in improving the permeability of macroporous SiC ceramics. The growth

of large platelet SiC grains generally accompanies the growth of pores, which also contributes to the increased permeability.

The permeabilities of the 0A7AY and 1A7AY samples were $1.3 \times 10^{-12}\,m^2$ and $1.0 \times 10^{-12}\,m^2$, respectively. Like the specific flow rate, the addition of more Al_2O_3–Y_2O_3 additive resulted in decreased permeability of the macroporous SiC ceramics because of the decreased porosity and decreased pore size.

In summary, the permeability of macroporous SiC ceramics is dependent on both porosity and microstructural characteristics. However, the development of large platelet SiC grains is very effective in increasing the permeability of macroporous SiC ceramics at an equivalent porosity.

4. Conclusions

By adjusting the initial α-SiC content in the processing of macroporous SiC ceramics, the SiC grain morphology can be controlled from equiaxed to large platelet grains. Large platelet α-SiC grains were obtained from β powder or a mixture of α/β powders containing small (≤10%) amounts of α powders by sintering at 1950 °C for 4 h.

The flexural strength increased with increasing α-phase content and showed a maximum strength of 26 MPa at a porosity of 56% when the starting material contained 100% α-SiC particles. In contrast, the toughness maximum ($0.42\,MPa\,m^{1/2}$) occurred when the α-SiC content was 3 wt% because of the optimum grain size (∼15 μm) of the platelet α-SiC grains. The growth of platelet SiC grains appears to eliminate or reduce the contribution of the crack-tip blunting mechanism operating in porous ceramics, resulting in little contribution to toughening.

The permeability of macroporous SiC ceramics is dependent on both the porosity and microstructural characteristics. However, the development of large platelet SiC grains was very effective in increasing the permeability of the macroporous SiC ceramics at an equivalent porosity. The specific flow rate at a Δp of 15 psi and the permeability of macroporous SiC ceramics fabricated from β-SiC ceramics with 5 wt% Al_2O_3–Y_2O_3 additives (porosity ∼58%) were $23.3\,L/min/cm^2$ and $1.9 \times 10^{-12}\,m^2$, respectively.

Acknowledgement

This study was supported by the Mid-career Researcher Program through National Research Foundation of Korea (NRF) grant (No. 2010-0027502) funded by the Korea government (MEST).

References

1. Kitaoka S, Matsushima Y, Chen C, Awaji H. Thermal cyclic fatigue behavior of porous ceramics for gas cleaning. *J Am Ceram Soc* 2004;**87**(5):906–13.
2. Adler J. Ceram diesel particulate filter. *Int J Appl Ceram Technol* 2005;**2**(6):429–39.
3. Wilkes TE, Young ML, Sepulveda RE, Dunand DC, Faber KT. Composites by aluminum infiltration of porous silicon carbide derived from wood precursors. *Scripta Mater* 2006;**55**:1083–6.
4. Colombo R. Conventional and novel processing methods for cellular ceramics. *Phil Trans R Soc A* 2006;**364**:109–24.
5. Nagano T, Sato K, Saitoh T, Iwamoto Y. Gas permeation properties of amorphous SiC membranes synthesized from polycarbosilane without oxygen-curing process. *J Ceram Soc Jpn* 2006;**114**(6):533–8.
6. Wach RA, Sugimoto M, Yoshikawa M. Formation of silicon carbide membrane by radiation curing of polycarbosilane an polyvinylsilane and its gas separation up to 250 °C. *J Am Ceram Soc* 2007;**90**(1): 275–8.
7. Yao X, Tan S, Zhang X, Huang Z, Jiang D. Low-temperature sintering of SiC reticulated porous ceramics with MgO–Al_2O_3–SiO_2 additives as sintering aids. *J Mater Sci* 2007;**42**:4960–6.
8. Vogt UF, Gyorfy L, Herzog A, Graule T, Plesch G. Macroporous silicon carbide foams for porous burner applications and catalyst supports. *J Phys Chem Solids* 2007;**68**:1234–8.
9. Ding S, Zeng YP, Jiang D. Gas permeability behavior of mullite-bonded porous silicon carbide ceramics. *J Mater Sci* 2007;**42**:7171–5.
10. Fukushima M, Zhou Y, Yoshizawa YI, Hirao K. Water vapor corrosion behavior of porous silicon carbide membrane support. *J Eur Ceram Soc* 2008;**28**:1043–8.
11. Fukushima M, Zhou Y, Yoshizawa YI. Fabrication and microstructural characterization of porous silicon carbide with nano-sized powders. *Mater Sci Eng B* 2008;**148**:211–4.
12. Park YH, Park JS, Hinoki T, Kohyama A. Development of manufacturing method for NITE-porous SiC ceramics using decarburization process. *J Eur Ceram Soc* 2008;**28**:657–61.
13. Fukushima M, Zhou Y, Yoshizawa YI. Fabrication and microstructural characterization of porous SiC membrane supports with Al_2O_3–Y_2O_3 additives. *J Membrane Sci* 2009;**339**:78–84.
14. Liu S, Zeng YP, Jiang D. Effects of CeO_2 addition on the properties of cordierite-bonded porous SiC ceramics. *J Eur Ceram Soc* 2009;**29**:1795–802.
15. Chae SH, Kim YW, Song IH, Kim HD, Narisawa M. Porosity control of porous silicon carbide ceramics. *J Eur Ceram Soc* 2009;**29**: 2867–72.
16. Colombo R, Mera G, Riedel R, Soraru GD. Polymer-derived ceramics: 40 years of research and innovation in advanced ceramics. *J Am Ceram Soc* 2010;**93**(7):1805–37.
17. Fukushima M, Nakata M, Ohji T, Yoshizawa YI. Fabrication and properties of ultra highly porous silicon carbide by the gelation-freezing method. *J Eur Ceram Soc* 2010;**30**:2889–96.
18. Eom JH, Kim YW. Effect of additives on mechanical properties of macroporous silicon carbide ceramics. *Met Mater Int* 2010;**16**(3): 399–405.
19. Kumar BVM, Kim YW. Processing of polysiloxane-derived porous ceramics: a review. *Sci Tech Adv Mater* 2010;**11**:044303.
20. Locs J, Berzina-Cimdina L, Zhurinsh A, Loca D. Effect of processing on the microstructure and crystalline phase composition of wood derived porous SiC ceramics. *J Eur Ceram Soc* 2011;**31**:183–8.
21. Yamane H, Shirai T, Morito H, Yamada T, Hasegawa Y, Ikeda T. Fabrication of porous SiC ceramics having pores shaped with Si grain templates. *J Eur Ceram Soc* 2011;**31**:409–13.
22. Esposito L, Sciti D, Piancastelli A, Bellosi A. Microstructure and properties of porous β-SiC template from soft woods. *J Eur Ceram Soc* 2004;**24**:533–40.
23. Mouazer R, Mullens S, Thijs I, Luyten J, Buekenhoudt A. Silicon carbide foams by polyurethane replica technique. *Adv Eng Mater* 2005;**7**(12):1124–8.
24. Streitwieser DA, Popovska N, Gerhard H. Optimization of the ceramization process for the production of three-dimensional biomorphic porous SiC ceramics by chemical vapor infiltration (CVI). *J Eur Ceram Soc* 2006;**26**:2381–7.
25. Herzog A, Vogt U, Kaczmarek O, Klingner R, Richter K, Thoemen H. Porous SiC ceramics derived from tailored wood-based fiberboards. *J Am Ceram Soc* 2006;**89**(5):1499–503.
26. Ding S, Zhu S, Zeng Y, Jiang D. Effect of Y_2O_3 addition on the properties of reaction-bonded porous SiC ceramics. *Ceram Int* 2006;**32**: 461–6.

27. Zhang Z, Wang F, Yu X, Wang Y, Yan Y, Li K, et al. Porous silicon carbide ceramics produced by a carbon foam derived from mixtures of mesophase pitch and Si particles. *J Am Ceram Soc* 2009;**92**(1):260–3.
28. Jin YJ, Kim YW. Low temperature processing of highly porous silicon carbide ceramics with improved flexural strength. *J Mater Sci* 2010;**45**: 282–5.
29. Biasetto L, Colombo P, Innocentini MDM, Mullens S. Gas permeability of microcellular ceramic foams. *Ind Eng Chem Res* 2007;**46**:3366–72.
30. Song IH, Kwon IM, Kim HD, Kim YW. Processing of microcellular silicon carbide ceramics with a duplex pore structure. *J Eur Ceram Soc* 2010;**30**:2671–6.
31. Colombo P, Bernardo E, Biasetto L. Novel microcellular ceramics from a silicone resin. *J Am Ceram Soc* 2004;**87**(1):152–4.
32. Eom JH, Kim YW. Effect of template size on microstructure and strength of porous silicon carbide ceramics. *J Ceram Soc Jpn* 2008;**116**(10): 1159–63.
33. Kim YW, Mitomo M, Emoto H, Lee JG. Effect of initial α-phase content on microstructure and mechanical properties of sintered silicon carbide. *J Am Ceram Soc* 1998;**81**(12):3136–40.
34. Nader M, Aldinger F, Hoffmann MJ. Influence of the α/β-SiC phase transformation on microstructural development and mechanical properties of liquid phase sintered silicon carbide. *J Mater Sci* 1999;**34**: 1197–204.
35. Strecker K, Ribeiro S, Oberacker R, Hoffmann MJ. Influence of microstructural variation on fracture toughness of LPS-SiC ceramics. *Int J Ref Met Hard Mater* 2004;**22**:169–75.
36. Jones RL, Rowcliffe DJ. Use of notched bend beams to measure the toughness of ceramics. *Am Ceram Soc Bull* 1979;**58**(12):1195.
37. Kim YW, Mitomo M, Hirotsuru H. Microstructural development of silicon carbide containing large seed grains. *J Am Ceram Soc* 1997;**80**(1): 99–105.
38. Kim YW, Mitomo M. Fine-grained silicon carbide ceramics with oxynitride glass. *J Am Ceram Soc* 1999;**82**(10):2731–6.
39. Kim YW, Jin YJ, Eom JH, Song IH, Kim HD. Engineering porosity in silicon carbide ceramics. *J Mater Sci* 2010;**45**:2808–15.
40. Lin PK, Tsai DS. Preparation and analysis of a silicon carbide composite membrane. *J Am Ceram Soc* 1997;**80**(2):365–72.
41. Eom JH, Kim YW, Song IH, Kim HD. Microstructure and properties of porous silicon carbide ceramics fabricated by carbothermal reduction and subsequent sintering process. *Mater Sci Eng A* 2007;**464**:129–34.
42. Roh MH, Kim YW, Kim W, Nishimura T, Seo WS, Ko SI, et al. Effect of aluminum nitride-scandia content on the microstructural and mechanical properties of sintered silicon carbide ceramics. *Met Mater Int* 2009;**15**(6):937–41.
43. Eom JH, Kim YW, Song IH, Kim HD. Processing and properties of polysiloxane-derived porous silicon carbide ceramics using hollow microspheres as template. *J Eur Ceram Soc* 2008;**28**:1029–35.
44. Ding S, Zeng YP, Jiang D. Thermal shock resistance of in situ reaction bonded porous silicon carbide ceramics. *Mater Sci Eng A* 2006;**425**:326–9.
45. Kumar BVM, Eom JH, Kim YW, Song IH, Kim HD. Effect of aluminum hydroxide content on porosity and strength of porous mullite-bonded silicon carbide ceramics. *J Ceram Soc Jpn* 2011;**119**(5):367–70.
46. Lee SG, Kim YW, Mitomo M. Relationship between microstructure and fracture toughness of toughened silicon carbide ceramics. *J Am Ceram Soc* 2001;**84**(6):1347–53.
47. Kim JY, Kim YW, Mitomo M, Zhan GD, Lee JG. Microstructure and mechanical properties of α-silicon carbide sintered with yttrium–aluminum garnet and silica. *J Am Ceram Soc* 1999;**82**(2):441–4.
48. Zhou Y, Hirao K, Toriyama M, Yamauchi Y, Kanzaki S. Effects of intergranular phase chemistry on the microstructure and mechanical properties of silicon carbide ceramics densified with rare-earth oxide and alumina additions. *J Am Ceram Soc* 2001;**84**(7):1642–4.
49. Lee SG, Shim WH, Kim JY, Kim YW, Kwon WT. Effect of sintering-additive composition on fracture toughness of liquid-phase-sintered SiC ceramics. *J Mater Sci Lett* 2001;**20**:143–6.
50. Deng ZY, She J, Inagaki Y, Yang JF, Ohji T, Tanaka Y. Reinforcement by crack-tip blunting in porous ceramics. *J Eur Ceram Soc* 2004;**24**:2055–9.
51. Kaul VS, Faber KT, Sepulveda R, Arellano Lopez AR, Martinez-Fernandez J. Precursor selection and its role in the mechanical properties of porous SiC derived from wood. *Mater Sci Eng A* 2006;**428**:225–32.